Finite-Element Investigation of Steel Plate Shear Walls with Infill Plates Strengthened by GFRP Laminate

Masoud Khazaei-Poul[1*] and Fariborz Nateghi-Alahi[2]

1. M.Sc. Graduated, Structural Engineering Research Center, International Institute of Earthquake Engineering and Seismology (IIEES), Iran,
* Corresponding Author; e-mail: m.khazaei.poul@gmail.com
2. Professor, Structural Engineering Research Center, International Institute of Earthquake Engineering and Seismology (IIEES), Iran

Received: 24/12/2011
Accepted: 02/12/2012

ABSTRACT

In composite steel plate shear walls system, steel web plates can be strengthened by adding a number of layers of fiber reinforced polymer laminate or concrete on one or both sides of the web plate. In this paper, nonlinear behaviour of strengthened steel plate shear wall by means of glass fiber reinforced polymer laminates have been numerically investigated. In that regard, the tested ½ scaled one-story un-stiffened steel plate shear walls have been selected and simulated using finite element method, based on the available experimental data in the literature. Non-linear large displacement analyses on the finite element model have been carried out and the results presented. The shear capacities and hysteresis curves of the experimental and numerical unstiffened steel plate shear wall are compared. It is found that the simulation outcomes have showed good agreement with the experimental results. After calibration of the numerical model, steel web plate is strengthened by GFRP laminate, and effects of GFRP laminate on the seismic behavior of strengthened steel plate shear walls are investigated. The results indicate that with strengthening infill steel plate on the steel plate shear walls, yield strength, ultimate shear capacity, secant stiffness and cumulative dissipated energy of SPSWs can be significantly increased.

Keywords:
Composite; Steel plate shear wall; Glass fiber reinforced polymer; Finite element method; Hysteretic

1. Introduction

Steel Plate Shear Wall (SPSW) system have significant advantage over many other systems in term of cost, primarily, substantial ductility, high initial stiffness, fast pace of construction, and the reduction in seismic mass [1]. SPSW system can be used in different configurations, such as:

1. Unstiffened steel plate shear wall;
2. Stiffened steel plate shear wall;
3. Composite steel plate shear wall.

Unstiffened-SPSW is the basis for SPSW systems. Unstiffened web plate has negligible compression strength and shear buckling occurs at low levels of loading. Lateral load are resisted through diagonal tension in the web plate. Stiffened web may also be used to increase shear buckling strength. In this type of SPSW, the shear strength is a combination of shear buckling strength and additional strength from diagonal tension action [2].

In high-rise buildings, drift control is much more difficult. Composite Steel Plate Shear Wall (C-SPSW) and strengthened SPSW are a lateral loading resistance system, which is adopted and used especially in high-rise buildings [2]. In C-SPSW system, steel web plate can be stiffened by adding concrete on one or both sides of the web plate. Concrete layers can improve load carrying capacity of SPSWs by

permitting utilization of the full yield strength of the infill plate. In addition, shear strength of the concrete is effective to increase capacity of system [1].

FRP laminates have high strength, high stiffness, light weight, flexibility to form in any shapes, and forms all kinds of shapes, easy to handle during construction, and excellent resistance to corrosion and environmental degradation. These superior mechanical properties of FRP laminate have made them effective alternatives for steel plates used for strengthening and upgrading steel structures [3-4].

For strengthening steel structures, CFRP have some disadvantages in comparison with GFRP. CFRP is generally corrosion resistant, but if it is in contact with metals, galvanic interaction between the two materials can take place. The use of GFRP has been proved to prevent galvanic corrosion and to achieve higher bonding strength [5]. In addition, failure strain of the GFRP laminates is more than CFRP laminates.

Steel infill plate can be strengthened by adding number of layers of fiber reinforced polymer laminate in both sides. In this type of C-SPSW, like unstiffened SPSW systems, strengthened steel plate has negligible compression strength and shear buckling occurs at low levels of loading. Lateral load are resisted through diagonal tension in the web plate. In C-SPSW, FRP laminate are effective to increase post buckling strength, initial and secant stiffness of the system [6]. The FRP layers can contribute more in resisting the shear stresses, extension of post buckling lines.

2. Literature Review

During the four last decades, many experimental and numerical researches on seismic performance of un-stiffened and stiffened SPSW have been carried out and these researches lead to better understanding of this lateral load resistant system. Wagner [7] is the first researcher who used a complete and uniform tension fields to determine the shear strength of a panel with rigid flanges and very thin web, and inferred that the shear buckling of a thin aluminum plate supported adequately on its edges does not constitute failure. Other researches were also conducted based on this idea to develop an analytical method for modeling of thin SPSW. Thorburn et al [8] developed a simple analytical method to evaluate the shear strength of unstiffened SPSWs with thin steel plates and introduced the strip model to represent the tension field action of a thin steel wall subjected to shear forces. Timler and Kulak [9] modified the formula for the angle of strips inclination with the column by the tests. Elaghy [10] experimentally investigated behavior of SPSW and proposed an analytical model to determine the behavior of thin steel plate shear walls. Berman and Bruneau [11] presented plastic analysis method based on the strip models as an alternative for the design of SPSW. This method has been implemented into the Canadian design codes for steel structure (CAN/CSA 2001) [12] and the AISC (2005b) seismic design specifications [13]. Sabouri-Ghomi et al [14] proposed Plate-Frame-Interaction (PFI) method to predict the shear behavior of the SPSWs. Kharrazi et al [15] presented modified plate frame interaction (M-PFI) method for use in the design of steel plate wall systems. Khazaei-Poul and Nateghi-Alahi [16] proposed an analytical model, the Composite-Plate Frame Interaction (C-PFI) method, to predict the shear behavior of the strengthened steel plate shear walls by FRP Laminate, and they showed that C-PFI method is able to properly predict the shear behavior of the C-SPSW systems.

Astaneh-Asl [17-18] performed experimental tests on the two specimens of three-story C-SPSW under cyclic loads. He showed that the concrete layer produces a better distribution of stress in the steel plate and developing tension field lines in a wider region. Rahai and Hatami [19], experimentally and numerically, investigated the effects of shear studs spacing variation, middle beam rigidity and the method of beam to column connection on the C-SPSW behavior.

Lubell et al [20] tested two single and one 4-story thin SPSWS under cyclic loading, compared the experimental results with the simplified tension field analytical models and found that the models can predict post-yield strength of the specimens well, with less satisfaction in the elastic stiffness results. Caccese et al [21] tested five one-fourth scale models of three-story into the effects of panel slender ratio and type of beam-to-column connection. They reported as the plate thickness increased, the failure mode was governed by column instability and the difference between simple and moment-resisting beam-to-column connection was small. Driver et al [22] tested a 4-story large-scale steel plate shear wall specimen with unstiffened panels

under cyclic loading to determine its behavior under an idealized severe earthquake event. Robert and Sabouri-Ghomi [23] conducted a series of 16 quasi-static loading tests on unstiffened steel plate shear panel with central opening. Vian et al [24] performed test on special perforated SPSW with reduced beam section anchor beams under cyclic loading and reported the perforated panel reduced the elastic stiffness and overall strength of the specimen by 15% as compared with the solid panel specimen.

Alinia [25] and Dastfan [26] studied the effect of surrounding members on the overall behavior of thin steel plate shear walls. His results show that the flexural stiffness of the surrounding members has no significant effect on elastic shear buckling or the post-buckling behavior of the shear walls.

On the other hand, several studies on the FRP strengthening of steel structures have been carried out. The "CIRIA Design Guide" [27] provided detailed design guidance for strengthening metallic structures using externally bonded FRP. Wright et al [28] experimentally investigated a joint between steel plates and FRP and found that, by increasing the thickness of the adhesive layer, the relative stress concentration level was reduced by 21%. Ekiz and El-Tawil [29] carried out an analytical and experimental research program conducted to investigate the buckling behavior of compressive steel braces strengthened with carbon fiber reinforced polymer (CFRP) laminates. Sen et al [30] studied on strengthening steel bridge sections using CFRP laminates. Moy et al [31] reported the upgrade of cast iron beams in the London underground systems by bonding CFRP plates to the tension flange. Deng and Lee [32] investigated the behavior of metallic beams reinforced with a bonded CFRP plate under static loading. Benachour et al [33] developed a new solution to predict both shear and normal interfacial stress in simply supported beams strengthened with bonded pre-stressed composite laminates. Studies on fatigue crack propagation in steel members strengthened by CFRP were carried out by [34-36]. Miller et al [37] tested two full-scale steel-CFRP composite girders under fatigue loading. Hollaway and Cadei [38] wrote an excellent state-of-the art review article on the problems encountered in plate bonding on to metallic structures, and discusses how these problems might be overcome. Zhao and Zhang wrote a comprehensive review article on the bond between steel and FRP, the strengthening of steel hollow section members, and fatigue crack propagation in the FRP-Steel system [4].

In this paper, a new type of SPSW system that strengthened steel plates by GFRP laminate are used as infill plate have been investigated numerically. In that regard, the tested $1/2$ scaled one-story un-stiffened steel plate shear walls have been selected and simulated using finite element method, based on the available experimental data in the literature. After calibration of finite element model with experimental model, steel infill plate in the numerical model has been strengthened by number of GFRP laminate layers and all specimens are subjected to quasi-static loading and results are presented.

3. Numerical Study

3.1. Basic Assumptions in the Analysis

The most common failure mode for FRP-strengthened steel plate is debonding and delamination of the FRP laminate [14]. In numerical models, several assumptions for modeling of FRP layers, bond between steel plate and FRP layer and bond between FRP layers are considered. They are summarized as follows:

- All FRP layers considered are linear elastic.
- Steel materials considered are nonlinear (multi-linear kinematic hardening)
- No slip is allowed at the interface of the bond (a perfect bond is considered at the bond between adhesive and steel infill plate interface and between FRP layers).
- Both a fiber reinforced polymer and adhesive in FEM model are considered as one layer.
- The adhesive layer is assumed to be thin so that stresses can be considered as constant through the layers thickness.

3.2. Validation and Verification of Results

To validate modeling, boundary conditions and loading procedures, two laboratory models of SPSWs at IIEES [39-40]were modeled and analyzed.

3.2.1. Verification of SPSW (Alavi-Nateghi 2011)

3.2.1.1. Model

SPSW1 specimen is $1/2$ scaled one-story speci-

men with around 2 m width and 1.5 m height, see Figure (1). In this model, un-stiffened web is used as infill plate. The boundary elements are similar, while the infill steel plate thickness is 1.5 mm. In this model, standard profile of HEB160 is used in the columns and beams, as boundary elements. At the top of specimen, an additional HEB160 was placed on the beam and welded along with the flanges, to better anchor the internal panel forces and to contribute with transferring loads of the horizontal jack to the specimen. Fish plates with dimensions of 70 mm × 5 mm were used all around the panel for connection of the infill plate to the boundary members [39].

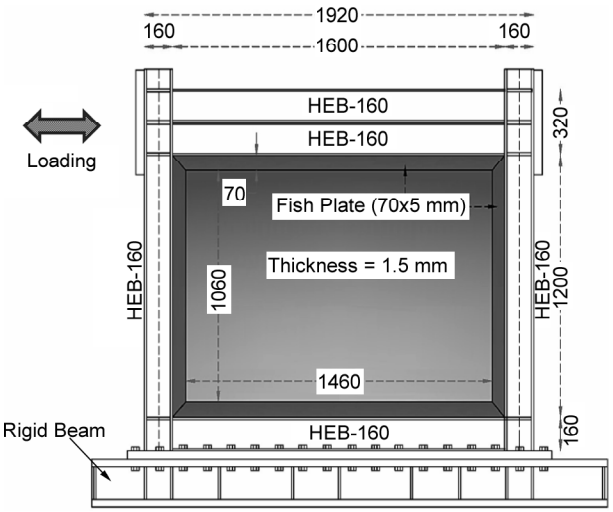

Figure 1. Details of the SPSW1 (Alavi and Nateghi).

3.2.1.2. Material Properties

Yield stress of steel infill plate, boundary elements and fish plate based on the mean of coupon tests are equal to 280 MPa, 340 MPa, and 340 MPa, respectively. The failure strains are approximately at 28% for all steel members. In Figure (2), strain-stress curves of materials, which are used in the FEM model, are shown.

3.2.1.3. Numerical Modeling

This SPSW is modeled in FEM software (ANSYS-V12).

a) Elements: In the finite element model, SHELL-181 was used for modeling of the steel infill plate and boundary elements. SHELL181 is a 4-noded 3-D element with 6 degrees of freedom at each node.

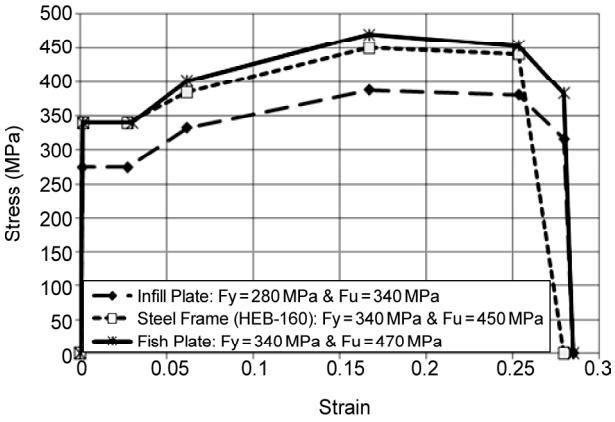

Figure 2. Material models in the FEM model.

The element possesses full nonlinear capabilities including large strain and allows defining 255 layers. In the analysis, multi-linear kinematic hardening model is assigned to boundary elements, infill plate, and fish-plate.

b) Optimum Dimension of Elements: Optimum dimension of elements by trial and error are selected, in condition that the smaller mesh size did not change considerably in the results of analysis, as shown in Figure (3).

c) Initial Imperfection: In the analysis, initial imperfection based on the first shape of elastic buckling is assigned to the numerical model. Initial imperfection based on first buckling mode of the SPSW1 is shown in Figure (4). Initial imperfection that is used in the analysis is less than 1% (5 mm). This amount of initial imperfection does not have a considerable influence on the nonlinear post-buckling behaviors. In reality, the thin infill plates upon mounting are already in a buckled shape due to fabrication process, welding distortion and assemblage.

3.2.1.3. Results

The numerical hysteretic and push-over load-displacement curves from the non-linear finite element modeling are presented and compared with experimental model in Figure (5). It is obtained that the used numerical method has been successful to estimate the actual shear capacity of the system and initial stiffness of the SPSW in comparison with the experimental results. The difference between obtained shear capacity in the numerical and experimental model is less than 5%. The differences between the numerical and experimental results

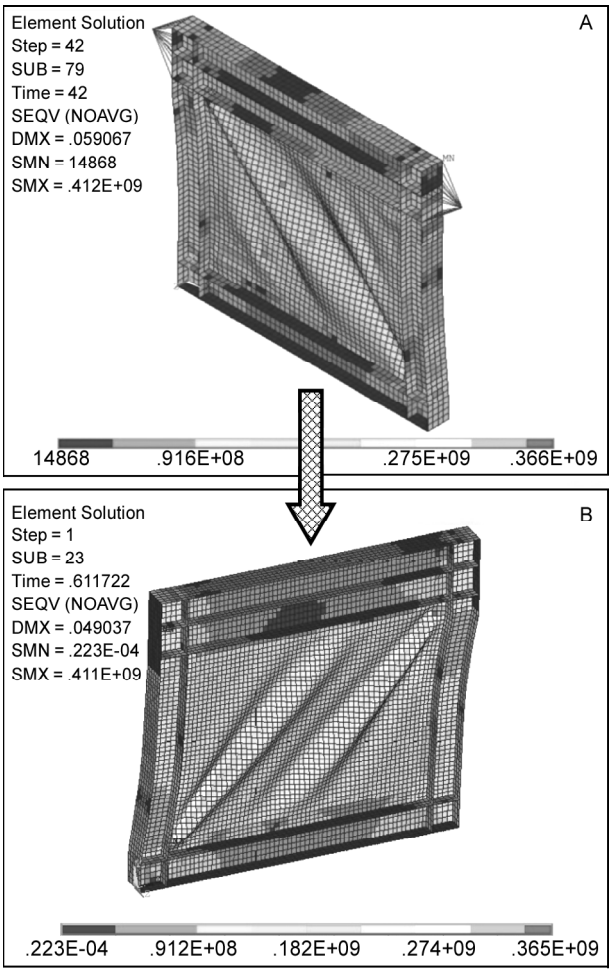

(a) FEM Models of SPSW1 with Different Mesh Size

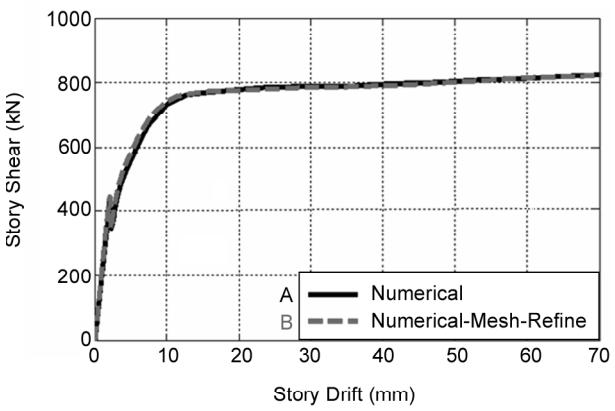

(b) Effect of Mesh Size in the Results of Analysis

Figure 3. The selection of optimum dimension of the elements by trial and error.

might have several reasons, for instance, effects of the initial imperfections, discretization error, numerical error and the remained residual stresses in the fabricated structural elements due to welding or hot-rolling, etc. The nonlinear results of Von-Mises yield criterion and out-of-plane deformation in 5.4 cm story drift are presented in Figure (6).

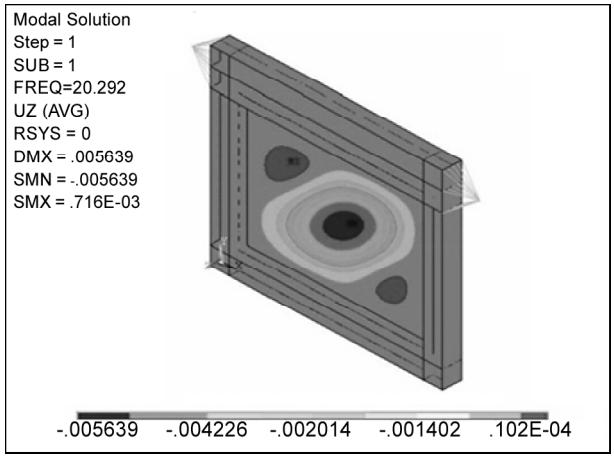

Figure 4. Initial imperfection based on first buckling mode of SPSW1.

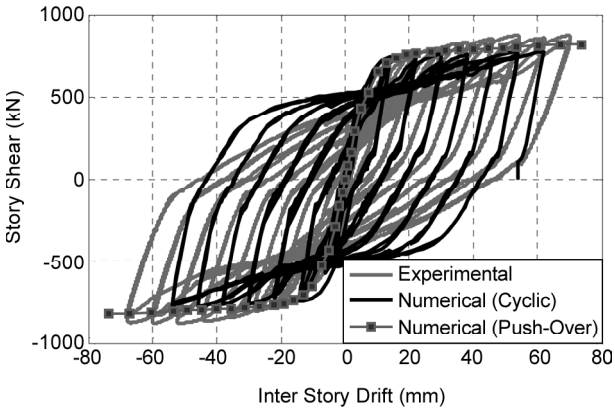

Figure 5. Good agreement between Numerical and experimental models.

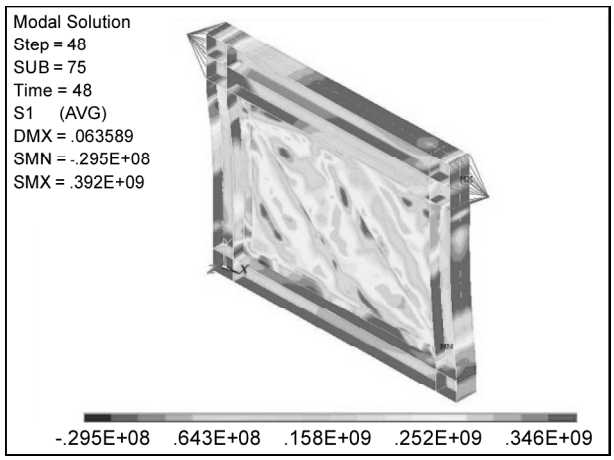

Figure 6. SPSW1,Von - Mises Stresses (Pa.)

3.2.2. Verification of Composite-SPSW [40]

Nateghi and Khazaei [40] experimentally studied cyclic behavior of strengthened steel plate shear panel by GFRP laminates. In this section, two models of their works (SPSP1 and CSPSP3) have

been modeled and analyzed in FEM software (ANSYS) and the results are compared with experimental results.

3.2.2.1. Models

SPSP1 and CSPSP3 specimens were scaled as a one-story steel shear panels, with hinge type connections of the boundaries at four corners. The depth and width of the all specimen were equal to 600 mm. Details of the experimental specimens are shown in Figure (7). In SPSP1, un-stiffened steel plate was used as infill plate, while in CSPSP3 steel infill plate was strengthened by two layer of GFRP laminate, Figures (8) and (9). Properties of infill plate in the experimental specimens are presented in Table (1).

3.2.2.2. Material Properties

Yield stress and young module of steel infill plate based on the mean of coupon tests are equal to 197 MPa and 204 GPa, respectively, and for boundary elements, those are equal to 310 MPa and 203 GPa, respectively. Summary of the mechanical properties

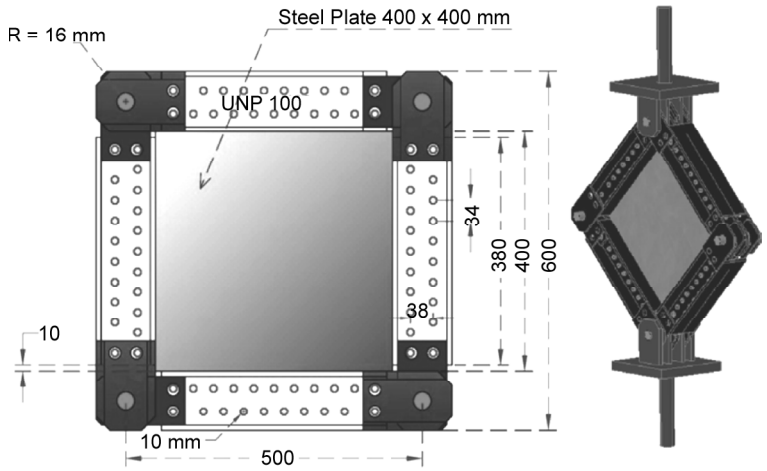

Figure 7. Details of the experimental specimens (mm) (Nateghi-Alahi and Khazaei 2012).

Table 1. Properties of infill plate in the experimental specimens.

Experimental Models	Number of Layers in Composite Infill Plate		Thickness of Laminate and Steel Infill Plate		Total Thickness of Infill Plate	Orientation of GFRP Layers	GFRP Type
	Steel Plate	GFRP Layer	Steel Plate	GFRP Layer			
SPSP1	1	0	0.9 mm	-	0.9 mm	-	-
CSPSP3	1	2	0.9 mm	0.508 mm	1.916 mm	45 # -45	SikaWrap®Hex430G

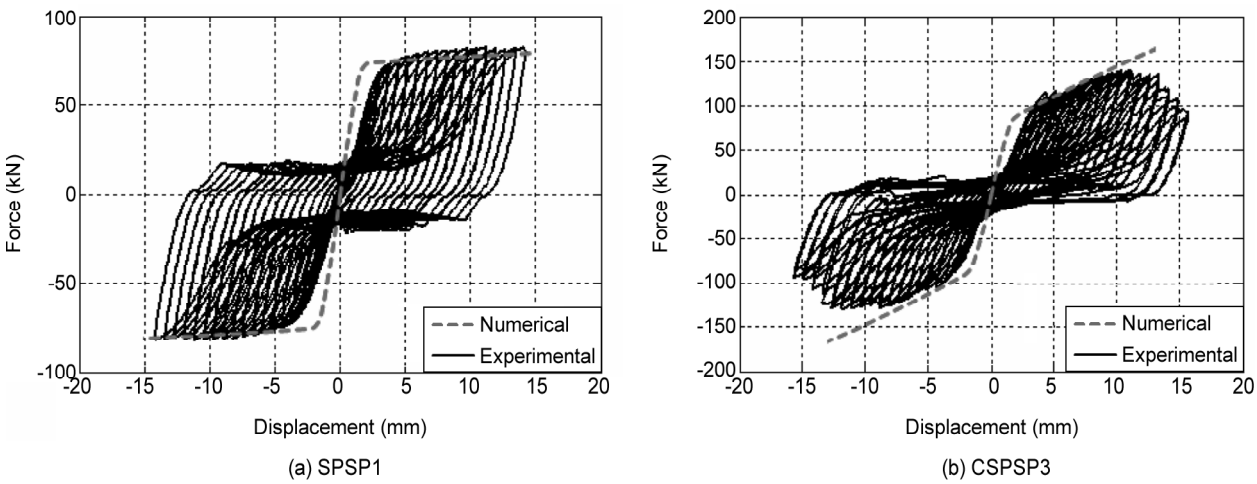

Figure 8. Comparative results between numerical and experimental models (good agreement).

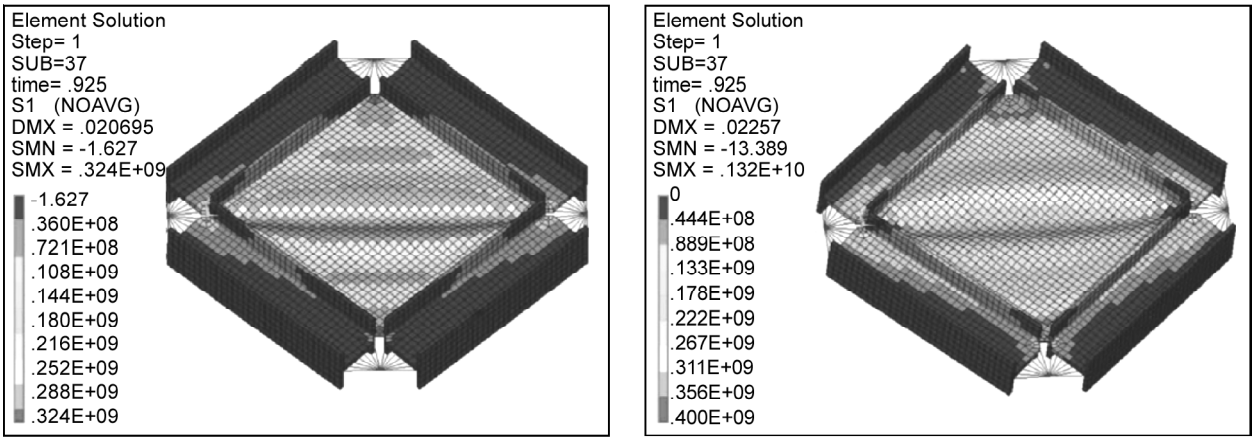

(a) SPSP1 (b) CSPSP3

Figure 9. Principal stress of the SPSP1 and CSPSP3 specimens (Pa.).

of the GFRP laminates are presented in Table (2). Comparison between strain-stress curves of the steel infill plate and the GFRP laminated layer in the main direction of the fibers is shown in Figure (10).

3.2.2.3. Numerical Modeling

Both boundary elements and infill plate were modeled by using nonlinear shell element (Shell-181). The shell section is used for modeling the composite infill plate. Two elements of the MPC184 and COMBIN7 were used to create hinge connections. The optimum dimension of the elements by trial and error was selected, under the condition that the smaller mesh size did not change the results of the analysis.

In the analysis, the multi-linear kinematic hardening model was assigned to the boundary elements and steel infill plate, while the GFRP layers were modeled as the orthotropic material. Tsai-Wu Failure Criterion, which allows nine failure stresses and three additional coupling coefficients, was assigned to the GFRP layers.

The numerical push-over load-displacement curves from the non-linear finite element modeling are presented and compared with experimental results in Figure (8). The results show that the used numerical method has been successful to estimate the actual shear capacity of the system and initial stiffness in comparison with the experimental results. The principal stresses of SPSP1 and CSPSP3 are presented in Figure (9).

Table 2. Mechanical properties of the Cured Laminate Properties of SikaWrap® Hex 430G with Sikadur 330 Epoxy.

Tensile Modulus		Tensile Strength	
Ex (GPa)	Ey (GPa)	Tx (MPa)	Ty (MPa)
26.49	7.07	537	23

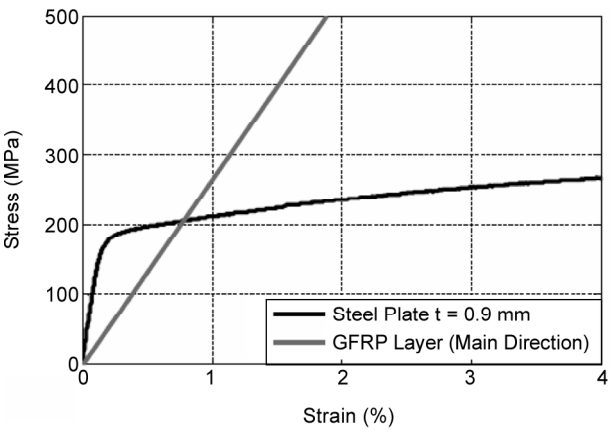

Figure 10. Strain-stress curves of steel infill plate and GFRP laminated layer in the direction of the fibers.

3.3. Composite Steel Plate Shear Walls Analysis

In the previous section, verification of the numerical method with an experimental model has been carried out. In this study, steel infill plate with thickness of 1.5 mm has been strengthened by numbers of GFRP layers with different orientations of GFRP layers. The methods of arranging the FRP laminates on the infill steel plate are shown in Figure (11). Infill plate is strengthened in four ways. Fiber-orientation angle plays an important role in the increase of the plate strength. This is due to FRP having high strength in the fiber direction, and low strength in the direction perpendicular to the fiber. Optimum performance from longitudinal fibers can be obtained if the

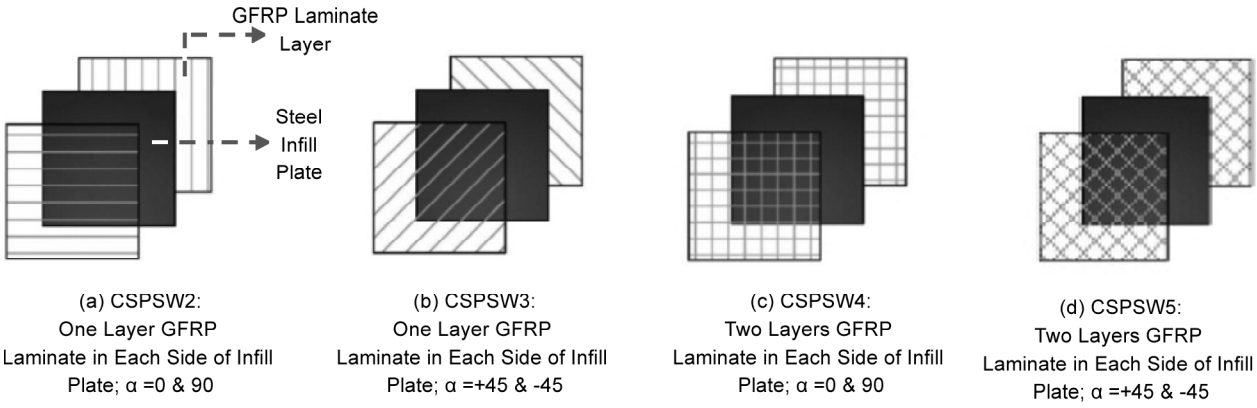

Figure 11. Different types of strengthening of infill steel plate by GFRP layers.

load is applied along its direction. The slightest shift in the angle of loading may drastically reduce the strength of the composite.

Details of the numerical models are summarized in Table (3). Composite steel infill plate in the CSPSW2 and CSPSW3 specimens are consisted of steel plates with a thickness of 1.5 mm that are strengthened by one layer of GFRP laminate in each side. In these specimens, total thicknesses of composite steel infill plate are equal to 3.5 mm. In the CSPSW2 specimen principal orientation of GFRP laminates (the direction at which the laminate has maximum amount of strength and young modules) are oriented horizontally and vertically ($\alpha = 0$ & 90) with respect to the horizontal beam as shown in Figure (11a). In the CSPSW3 specimen, principal orientation of GFRP laminates are oriented in a +45 and -45 degrees inclination with respect to the horizontal beam as shown in Figure (11b). Composite steel infill plates in the CSPSW4 and CSPSW5 specimens are consisted of steel infill plates with thickness of 1.5 mm that are strengthened by two layers of GFRP laminate at each side. In these specimens, total thicknesses of composite steel infill plate are equal to 5.5 mm.

In the CSPSP4 specimen, like CSPSW2 specimen, principal orientation of GFRP laminates are oriented horizontally and vertically with respect to the horizontal beam as shown in Figure (11c). In the CSPSP5 specimen, like CSPSW3 specimen, principal orientation of GFRP laminates are oriented in a +45 and -45 degrees inclination with respect to the horizontal beam as shown in Figure (11d).

In the finite element models, SHELL-181 is used for modeling of the GFRP layers and infill plate. SHELL181 is a 4-node 3-D element with 6 degrees of freedom at each node. The element has full nonlinear capabilities including large strain and allows defining 255 layers. Shell section is used for modeling composite infill layers (GFRP layers that are attached to infill steel plate). Kinematic hardening plasticity model has been utilized with multilinear kinematic hardening material model for the mild steel material. The GFRP layers are modeled with orthotropic material. Mechanical properties of the GFRP laminate, such as young's modules and tensile strength are summarized in Table (4). Tsai-Wu Failure Criterion, which allows nine failure stresses and three additional coupling coefficients, is assigned to GFRP layers.

Table 3. Details of the numerical models.

Numerical Models	Number of Layers in Composite Infill Plate		Thickness of Laminate and Steel Plate		Orientation of GFRP	GFRP NO
	Steel Plate	GFRP Layer	Steel Plate	GFRP Layer		
SPSW1	1	0	1.5 mm	1 mm	-	-
CSPSW2	1	2	1.5 mm	1 mm	0 & 90	SikaWrap® Hex 430G
CSPSW3	1	2	1.5 mm	1 mm	+45 & -45	SikaWrap® Hex 430G
CSPSW4	1	4	1.5 mm	1 mm	0 & 90	SikaWrap® Hex 430G
CSPSW5	1	4	1.5 mm	1 mm	+45 & -45	SikaWrap® Hex 430G

Table 4. Mechanical properties of GFRP laminate.

GFRP	Tensile Modulus		Tensile Strength	
	Ex (Mpa)	Ey (Mpa)	Tx (Mpa)	Ty(Mpa)
SikaWrap® Hex 430G	26493	7069	537	23

3.3.1. Loading

The specimens are subjected to quasi-static cyclic loading in compliance with ATC-24 (1992) test protocol. A similar load protocol was used for all numerical specimens. In Figure (12), the load protocol that was applied on the all specimens is provided.

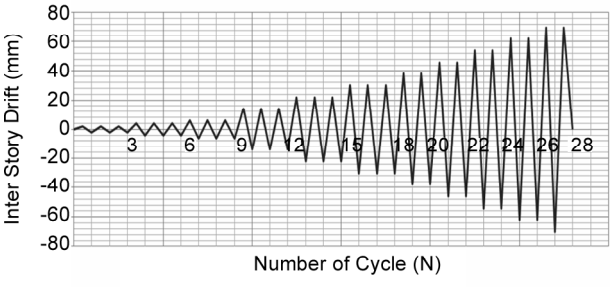

Figure 12. Load protocol based on ATC-24 (1992).

3.3.2. Discussion of Results

After verification, the SPSW1 specimen has been strengthened by number of GFRP layers with different orientation. Hysteresis load-displacement curves for the specimens are presented in Figure (13). As shown in this figure, very good hysteretic performance of SPSWs and CSPSWs can be noticed.

i. Ultimate shear strength: Ultimate shear strength of the SPSW1, CSPSW2, CSPSW3, CSPSW4, CSPSW5 are equal to 776 kN, 1012 kN (30% increase in the shear strength), 1181 kN (52% increase in the shear strength), 1193 kN (54% increase in the shear strength) and 1365 kN (76% increase in the shear strength), respectively. Accordingly, if principal orientation of GFRP laminates is oriented in the direction of tension fields, the shear strength in the specimens reaches the maximum possible value.

Therefore, fiber orientation is an important variable in the ultimate shear strength of the C-SPSW. The structural capacity of FRP laminate can be tailored and maximized by aligning fibers along the optimal orientation. For C-SPSW, it is well established

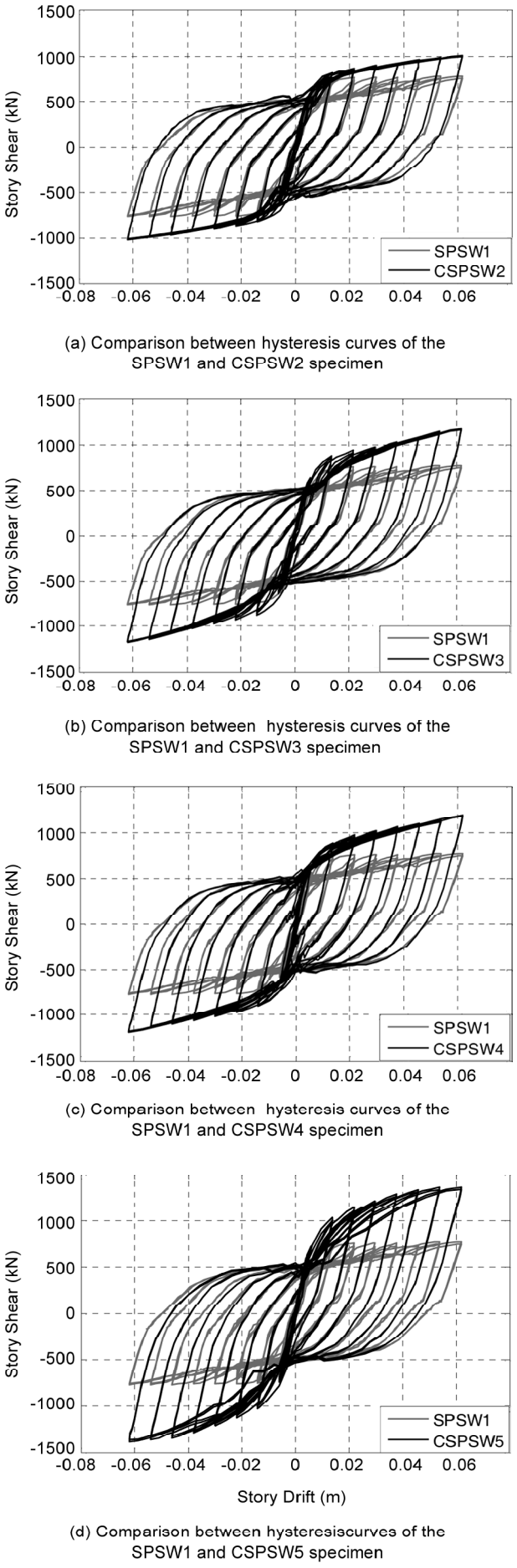

Figure 13. Hysteresis curve of the numerical specimens.

that fibers should be aligned along the direction of tension field. In this state, maximum shear strength are provided by FRP laminate.

ii. Cumulative Dissipated Energy: Cumulative (hysteretic) dissipated energy is the summation of dissipated energy experienced by the specimen during the test. This parameter is one of the most important characteristics affecting the seismic performance of the C-SPSW system. In Figure (14) and Figure (15), the comparison in terms of cumulative (hysteretic) dissipated energy versus drift of all the specimens is provided. In the all specimens, with increasing drift, cumulative dissipated energy of the specimens was increased. Cumulative dissipated energy in the all strengthened specimens is larger than un-strengthened specimen (SPSW1). At the 2.53 % drift, cumulative dissipated energy of the CSPSW2, CSPSW3, CSPSW4, and CSPSW5 specimens have been increased 19.5%, 23%, 31%, and 32%, respectively. As it can be seen, the amount of absorbed energy in CSPSW2 and CSPSW3, and also in CSPSW4 and CSPSW5 are close each other. However, if the principal orientation of GFRP laminates is oriented in the direction of tension fields, the cumulative dissipated energy in specimens is a little more. Therefore, as the results show, fiber orientation is not a substantial variable in the cumulative dissipated energy of the C-SPSW.

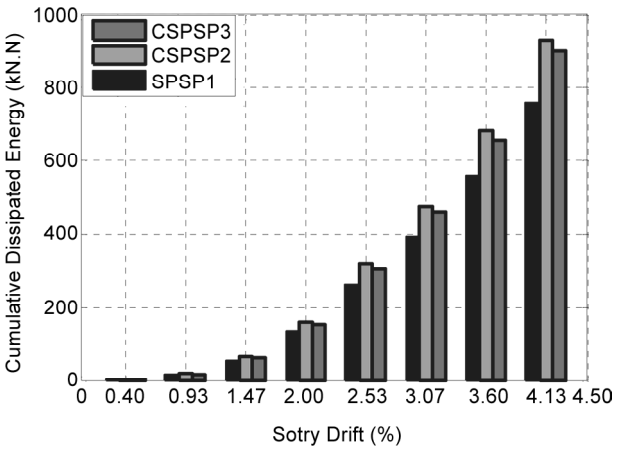

Figure 14. Cumulative dissipated energy of the SPSW1, CSPSW2, and CSPSW3.

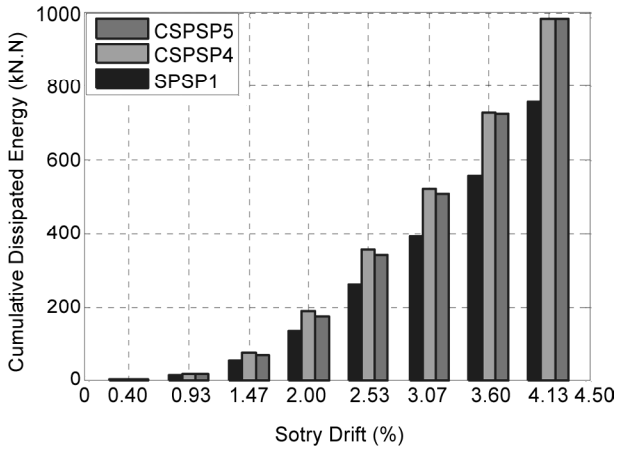

Figure 15. Cumulative dissipated energy of the SPSW1, CSPSW4, and CSPSW5.

iii. Secant Stiffness: In Figure (16), the comparison in terms of Secant stiffness versus drift of the all specimens is provided. The secant stiffness is calculated based on the tangent stiffness of the last cycle of each displacement increment as shown in Appendix I.

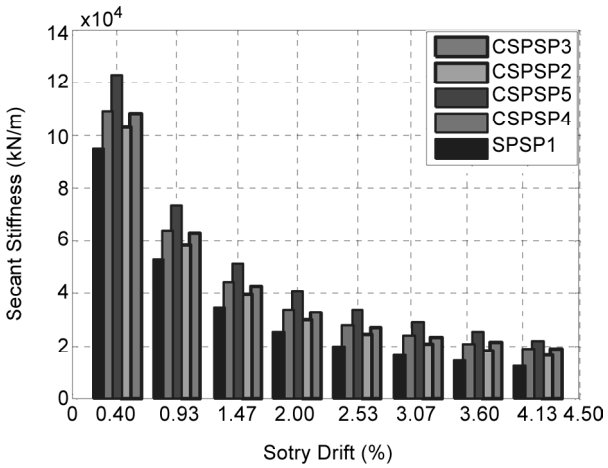

Figure 16. Secant stiffness of the specimens.

In order to control story drift, secant stiffness is one of the important seismic parameters. Secant stiffness in the all strengthened specimens is larger than the un-strengthened specimen (SPSW1). The results show that the orientation of GFRP laminates have a significant effect on the secant stiffness of the specimen. At the 2.53% drift, secant stiffness of the CSPSW2, CSPSW3, CSPSW4, and CSPSW5 specimens have been increased 28%, 47%, 47%, and 76%, respectively. Accordingly, if principal orientation of GFRP laminates is oriented in the direction of tension fields, the secant stiffness in specimens reaches the maximum possible value.

iv. Equivalent viscous damping ratio: The classical expression is considered for the assessment of viscous damping coefficient ξ_{eq} [41]

$$\xi_{eq} = \xi_0 + \xi_{hyst} \quad (1)$$

where ξ_0 corresponds to the initial damping in the elastic range and ξ_{hyst} corresponds to the equivalent viscous damping ratio that represents the dissipation due to nonlinear (hysteric) behavior. Method of Calculating ξ_{hyst} is presented in the appendix I. In Figure (17), the comparison in terms of equivalent viscous damping ratio of the all specimens is provided. Numerical results show that by strengthening infill plate, equivalent viscous damping ratios of system was decreased. The SPSW1 specimen has a maximum equivalent viscous damping ratio between all specimens. On the other hand, the CSPSW5 specimen has a minimum equivalent viscous damping ratio between all specimens. Numerical Results show that if principal orientations of the GFRP layers lie in direction of tension field lines, equivalent viscous damping ratio of the C-SPSW will be decreased.

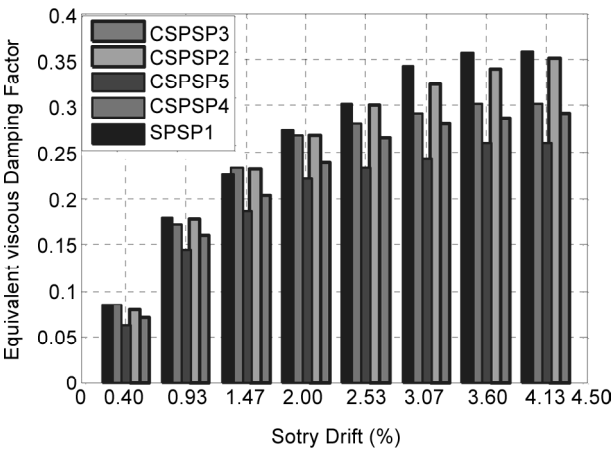

Figure 17. Equivalent viscous damping ratio of the specimens5.

Figures (18) to (21) depict the corresponding Von-Mises stress distribution at 4% drift. In the steel plate shear walls overturning moments could be caused instability in the SPSWs columns and local buckling in them. As shown, significant plastic deformations have taken place in the top of compression column. Adding GFRP laminate increased the amount of overturning moments, and as a result of that local buckling of compression column occurs in strengthened C-SPSWs specimens with four layers of GFRP laminate. Large plastic deformations observed in the CSPSW4 specimen and in the CSPSW5 specimen at compression column, Figures (20) and (21), but this phenomena in the SPSW2, and SPSW3 specimens are inconsiderable.

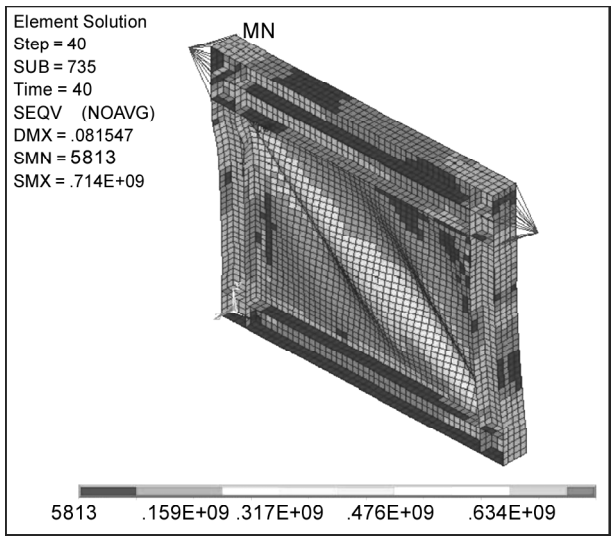

Figure 18. CSPSW2, Von-Mises Stresses (Pa.).

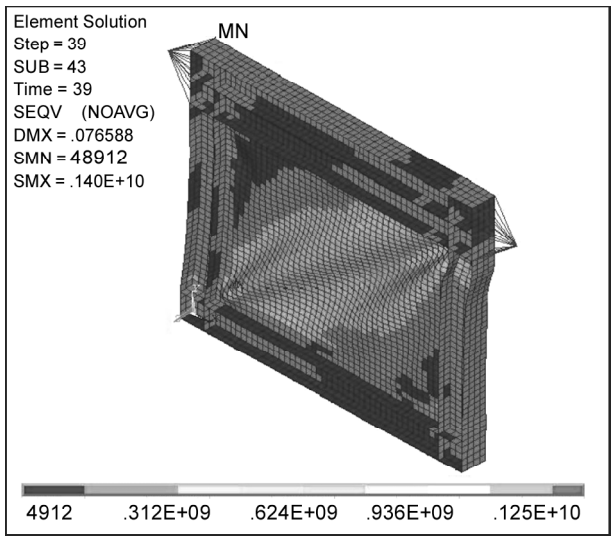

Figure 19. CSPSW3, Von-Mises Stresses (Pa.).

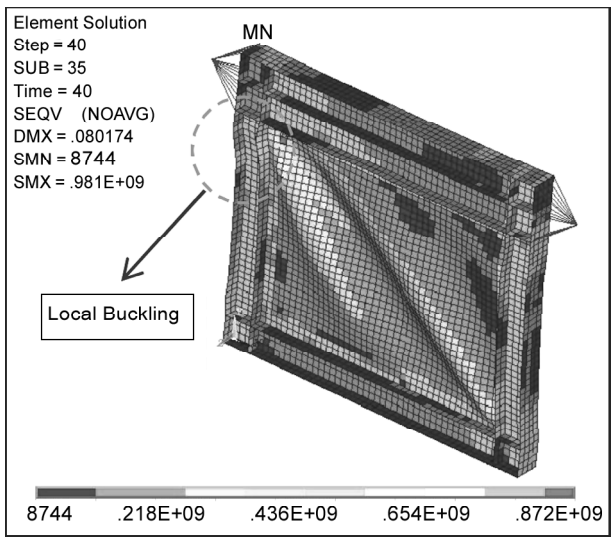

Figure 20. CSPSW4, Von-Mises Stresses (Pa.).

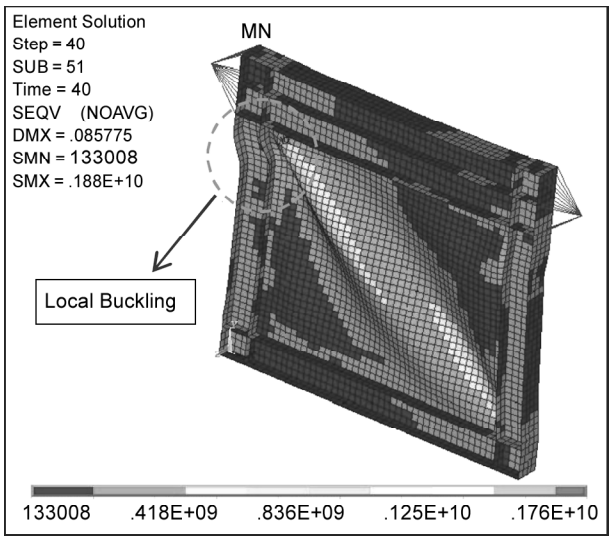

Figure 21. CSPSW5, Von-Mises Stresses (Pa.)

4. Conclusions

In this study, nonlinear behavior of the composite steel plate shear walls by means of glass fiber reinforced polymer laminates have been numerically investigated.The main results can be summarized as follows:

- The shear capacities and hysteresis curves of the experimental and numerical unstiffened steel plate shear wall are compared. It is found that the simu lation outcomes showed good agreement with the experimental results.
- If steel infill plate strengthens by GFRP layers, yield and ultimate strength of the C-SPSW will significantly increase. Fiber orientation is an important variable in the shear strength. If principal orientation of GFRP laminates is oriented in the direction of tension fields, the shear strength will increase.
- If steel infill plate strengthens by GFRP layers, initial and secant stiffness of the C-SPSW will significantly increase. If principal orientation of GFRP laminates is oriented in the direction of tension fields, the initial and secant stiffness will increase.
- Cumulative dissipated energy in the all strengthened specimens is larger than un-strengthened specimen. Fiber orientation is not a substantial variable in the cumulative dissipated energy of the C-SPSW. However, if the principal orientation of GFRP laminates is oriented in the direction of tension fields, the cumulative dissipated energy in specimens are a little more.
- Equivalent viscous damping ratio in the strengthened specimens is less than un-strengthened specimen. Results show that if principal orientations of the GFRP layers lie in direction of tension fields, equivalent viscous damping ratio of the composite SPSP will be decreased.
- Fiber orientation is an important variable on the behavior of the C-SPSW.

Acknowledgment

Authors would like to thank IIEES for their technical support.

References

1. Astaneh-Asl, A. (2001). Seismic behaviour and design of Steel Shear Walls, Steel TIPS Report, Structural Steel Educational Council, Moraga, CA.

2. Sabelli, R. and Bruneau, M. (2007). Design Guide 20: Steel Plate Shear Walls, American Institute of Steel Construction. Chicago, IL, USA.

3. Haghani, R. (2010). Analysis of Adhesive Joints Used to Bond FRP Laminates to Steel Members-A Numerical and Experimental Study, *Construction and Building Materials*, **24**(11), 2243-2251

4. Zhao, X-L. and Zhang, L. (2007). State-of-the-Art Review on FRP Strengthened Steel Structures, *Engineering Structures*, **29**(8), :1808-23.

5. Photiou, N.K., Hollaway, L.C., and Chryssanthopoulos, M.K. (2002). Strengthening of an Articially Degraded Steel Beam Utilising a Carbon/Glass Composites System, *Proceedings of the 2nd International Conference on Advances Polymer Composites for Structural Applications in Construction*, Guildford, UK, Woodhead Publishing Limited.

6. Khazaei-Poul, M. and Nateghi-Alahi, F. (2011). Behavior of Strengthened Steel Plate Shear Wall by FRP Laminate, M.Sc. Thesis, International Institute of Earthquake Engineering and Seismol ogy (IIEES), Iran.

7. Wagner, H. (1931). Flat Sheet Metal Girders with Very thin Webs, Part I, General Theories and Assumptions, Tech. Memo. National Advisory Committee for Aeronautics, Washington D.C., No. 604.

8. Thorburn, L.J., Kulak, G.L., and Montgomery, C.J. (1983). Analysis of Steel Plate Shear Walls, Structural Engineering Report 107, Edmonton (Alberta, Canada).

9. Timler, P.A. and Kulak, G.L. (1983). Experimental Study of Steel Plate Shear Walls, Structural Engineering Report, University of Alberta, Canada, No. 114.

10. Elgaaly M. (1998). Thin Steel Plate Shear Walls Behavior and Analysis, Thin Walled, *Structures*, **32**, 151-180

11. Berman, J.W. and Bruneau, M. (2003). Plastic Analysis and Design of Steel Plate Shear Walls, *Journal of Structural Engineering*, **129**(11), 1148-1156.

12. CAN/CSA S16-2001 (2001). Limit State Design of Steel Structures, Canadian Standards Association, Willowdale, ON., Canada.

13. AISC (2005b). Specifications for Structural Steel Buildings, American Institute of Steel Construction, Chicago, IL., USA.

14. Sabouri-Ghomi, S., Ventura, C., and Kharrazi H.K. (2005). Shear Analysis and Design of Ductile Steel Plate Walls, *Journal of Structural Engineering*, **131**(6).

15. Kharrazi, M.H.K. (2005). Rational Method for Analysis and Design of Steel Plate Walls, Ph.D. Dissertation, Vancouver (Canada), University of British Columbia.

16. Khazaei-Poul, M. and Nateghi-Alahi, F. (2012). Theoretical and Numerical Study on the Strengthened Steel Plate Shear Walls by FRP Laminates, International Journal of Engineering, IJE TRANSACTIONS C: ASPECTS, **25**(1).

17. Astaneh-Asl, A. (1998-2000). Seismic Studies of Innovative and Traditional Composite Shear Walls, Research Project In-Progress, Dept. of Civil and Env. Engineering, Univ. of California, Berkeley.

18. Astaneh-Asl, A. (2001). Cyclic Tests of Steel Shear Walls, Research Project, Berkeley: Dept. of Civil and Environmental Engineering, Univ. of California.

19. Rahai, A. and Hatami, F. (2009). Evaluation of Composite Shear Wall Behavior under Cyclic Loadings, *Journal of Constructional Steel*, **65**(7), 1528-37.

20. Lubell, A.S., Prion, H.G.L., Ventura, C.E., and Rezai, M. (2000). Unstiffened Steel Plate Shear Wall Performance under Cyclic Loading, *Journal of Structural Engineering*, **126**(4), 453-460.

21. Caccese, V., Elgaaly, M., and Chen, R.(1993). Experimental Study of Thin Steel-Plate Shear Walls under Cyclic Load, *ASCE Journal of Structural Engineering*, **119**(2), 573-587.

22. Driver, R.G., Kulak, G.L., and Kennedy, D.J.L. (1998). Cyclic Tests of Four-Story Steel Plate Shear Wall, *ASCE Journal of Structural Engineering*, **124**(2), 112-120.

23. Sabouri-Ghomi, S. and Roberts, T.M. (1992). Nonlinear Dynamic Analysis of Steel Plate Shear Walls Including Shear and Bending Deformations, E*ngineering Structures*, **14**(5), 309-317.

24. Vian, D., Bruneau, M., Tsai, K.C., and Lin, Y.C. (2009). Special Perforated Steel Plate Shear Walls with Reduced Beam Section Anchor Beams, I: Experimental Investigation, *Journal of Structural Engineering*, **135**(3), 211-220.

25. Alinia, M.M. (2005). A Study into Optimization of Stiffeners in Plates Subjected to Shear Loading, *Thin-Walled Structures*, **43**(5), 845-860.

26. Alinia, M.M. and Dastfan, M. (2006). Behaviour of Thin Steel Plate Shear Walls Regarding Frame Members, *Journal of Constructional Steel Research*, **62**, 730-738.

27. Cadei, J.M.C., Stratford, T.J., Hollaway, L.C., and Duckett, W.G. (2004). Strengthening Metallic Structures Using Externally Bonded Fibre Reinforced Composites, London, CIRIA.

28. Wright, P.N.H., Wu, Y., and Gibson, A.G. (2000). Fiber Reinforced Composite-Steel Connections for Transverse Ship Bulkheads, *Plastic Rubber Compos.*, **29**(10), 549-557.

29. Ekiz, E. and El-Tawil, S. (2006). Inhibiting Steel Brace Buckling Using CFRP Wraps, *Proceedings of the Eighth National Conference on EQ*

Engineering, San Francisco.

30. Sen, R., Liby, L., and Mullins, G. (2001). Strengthening Steel Bridge Sections Using CFRP Laminates, *Compos. Part B- Eng.*, **32**(4), 309-322.

31. Moy, S.S.J., Barnes, F., and Moriarty, J. (1999). Structural Upgrading and Life Extension of Struts and Beams Using Carbon Fiber Reinforced Composite, *Proceedings of the Conference on Composites and Plastics in Construction*, Watford, UK, Building Research Establishment, Paper 15:1.

32. Jun, D., Marcus, M.K., and Lee, B. (2007). Behaviour under Static Loading of Metallic Beams Reinforced with a Bonded CFRP Plate, *Composite Structures*, **78**, 232-242.

33. Benachour, A., Benyoucef, S., Tounsi, A., and Adda-Bedia, E.A. (2008). Interfacial Stress Analysis of Steel Beams Reinforced with Bonded Prestressed FRP Plate, *Engineering Structures*, **30**(11), 3305-3315.

34. Colombi, P., Bassetti, A., and Nussbaumer, A. (2003). Analysis of Cracked Steel Members Reinforced by Pre-Stress Composite Patch, *Fatigue Fracture of Engineering Materials Structures*, **26**, 59-66.

35. Jones, S.C. and Civjan, S.A. (2003). Application of Fibre Reinforced Polymer Overlays to Extend Steel Fatigue Life, *Journal of Composites for Construction, ASCE*, **7**(4), 331-338.

36. Tavakkolizadeh, M. and Saadatmanesh, H. (2003). Fatigue Strength of Steel Girders Strengthened with Carbon Fiber Reinforced Polymer Patch, *Journal of Structural Engineering, ASCE*, **129**(2), 186-96.

37. Miller, T.C., Chajes, M.J., Mertz, D.R., and Hastings, J.N. (2001). Strengthening of a Steel Bridge Girder Using CFRP Plates, *ASCE J. Bridge Eng.*, **6**(6), 514-22.

38. Hollaway, L.C. and Cadei, J. (2002). Progress in the Technique of Upgrading Metallic Structures with Advanced Polymer Composites, Prog. Struct. Engng Mater, **4**, 131-148 (DOI: 10.1002/pse.112).

39. Alavi, E. and Nateghi, F. (2010). Experimental and Analytical Study on Boundary Elements Effects on Steel Plate Shear Walls Behavior, *12th European Conf. on Earthquake Engineering*, Paper No.45.

40. Nateghi-Alahi, F. and Khazaei-Poul, M. (2012). Experimental Study of Steel Plate Shear Walls with Infill Plates Strengthened by GFRP Laminates, *J. of Constructional Steel Research*, **78**, 159-172.

41. Roy, R., Craig, Jr, and Andrew, J.K. (2006). Fundamentals of Structural Dynamics, Second Edition, Published by John Wiley & Sons, Inc., Hoboken, New Jersey ISBN 13, 978-0-471-43044-5.

Appendix I [41]

1. E_D: Dissipated energy in each cycle that is equal to area of loops in each cycle, see Figure (22).
2. K_{sec}: Secant stiffness (based on Figure (22)):

$$K_{\sec} = \frac{\Delta F}{\Delta L} = \frac{F_{\max} - F_{\min}}{\Delta_{\max} - \Delta_{\min}} \tag{1}$$

3. Equivalent viscose damping ratio (ζ)(based on Figure (22)):

$$\zeta = \frac{1}{4\pi}\left(\frac{E_D}{E_S}\right) \tag{2}$$

$$Es = \frac{1}{8}(F_{\max} - F_{\min}) \times (\Delta_{\max} - \Delta_{\min}) \tag{3}$$

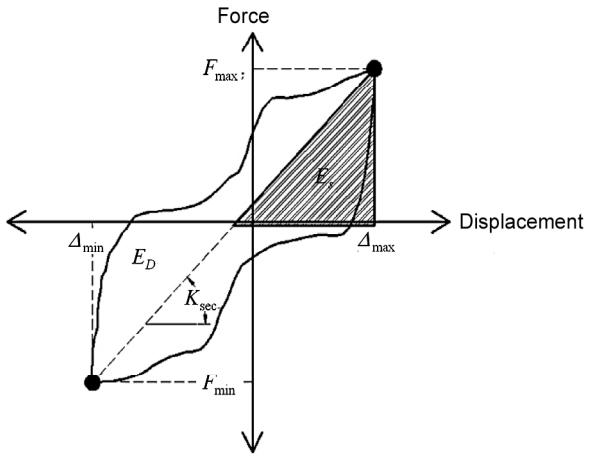

Figure 22. One loop of the hysteretic curves.